A Reversible NO-Triggered Multiple Metallaborane Cluster Fusion By Ligand Expulsion/Addition from $(PMe_2Ph)_4Pt_2B_{10}H_{10}$ to Afford $(PMe_2Ph)_8Pt_8B_{40}H_{40}$ and $(PMe_2Ph)_5Pt_4B_{20}H_{20}$.

Jonathan Bould,*[a] William Clegg,[b] Paul G. Waddell,[b] Josef Cvačka,[c] Michal Dušek,[d] and Michael G. S. Londesborough[a]

[a] Institute of Inorganic Chemistry of the Czech Academy of Sciences, Husinec-Řež, 250 68, Czech Republic

[b] Chemistry, School of Natural and Environmental Sciences, Newcastle University, Newcastle upon Tyne NE1 7RU, UK

[c] Institute of Organic Chemistry and Biochemistry of the Czech Academy of Sciences, Flemingovo nám. 2, CZ-166 10 Prague 6, Czech Republic

[d] Institute of Physics of the Czech Academy of Sciences, Na Slovance 2, 182 21 Prague, Czech Republic.

Abstract

The dimetallic boron hydride cluster, $(PMe_2Ph)_4Pt_2B_{10}H_{10}$ (**1**-Pt_2), is known to reversibly sequester small molecules (e.g. O_2, CO, and SO_2) across its Pt-Pt cluster vector. Here, we report the very different effect of the addition of nitric oxide (NO) to solutions of (**1**-Pt_2) that prompts the elimination of some of its phosphine ligands and the auto-fusion of the resultant $\{(PMe_2Ph)_xPt_2B_{10}H_{10}\}$ units to afford the metallaborane conglomerates $(PMe_2Ph)_8Pt_8B_{40}H_{40}$ (**2**-Pt_8, 38 %) and $(PMe_2Ph)_5Pt_4B_{20}H_{20}$ (**3**-Pt_4, 34 %). Single-crystal X-ray studies of these multi-cluster assemblies reveal the links between the clusters to be a combination of both Pt-Pt bonds and Pt-μH-B 2-electron, 3-center bonds in (**2**-Pt_8) and Pt-μH-B 2-electron, 3-center bonds in (**3**-Pt_4). For compound (**2**-Pt_8), the cluster assemblage can be effectively reversed by the addition of ethyl isonitrile (EtNC) to afford $(EtNC)_3(PMe_2Ph)_2Pt_2B_{10}H_{10}$ **4** in quantitative yield. The compounds were characterised by mass spectrometry, multi-element NMR spectroscopy and single-crystal X-ray diffraction studies.

Introduction

The reversible binding of small molecules on metal atoms, metal-metal vectors, and metal surfaces is used, both in nature and in industry, to overcome otherwise insurmountable thermodynamic barriers in chemistry. Examples of uses found for this type of interaction are numerous; the reversible uptake of dioxygen on the iron center in hemoglobin, and the catalytic conversion of carbon monoxide to

carbon dioxide on platinum surfaces, are two obvious examples. The dimetallic 12-vertex cluster series $(PMe_2Ph)_4MM'B_{10}H_{10}$ (MM' = Pt,Pt (**1**-Pt_2), Pt,Pd, Pd,Pd) has also been shown to sequester small molecular species with lone electron pairs, such as O_2, CO, SO_2 and EtNC across its metal-metal vector (Scheme 1).[1] Depending on the binding strength of these sequestered bridging ligands, and the identity of the metals, the captured small molecule may be removed either by purging with an inert gas and/or with gentle warming. In addition, UV irradiation of $(PMe_2Ph)_4(O_2)Pt_2B_{10}H_{10}$ or $(PMe_2Ph)_4(CO)Pt_2B_{10}H_{10}$ effects the release their sequestered O_2 or CO molecules with high quantum yields of 0.6.[1c] In this system, density functional theory calculations (DFT) have been shown to model well certain properties of the bridging ligands, such as the IR stretching frequency of CO,[1d] the μ-(C=N-R) angle of the bridging isonitrile,[1d] or the weaker bonding of SO_2 in $(PMe_2Ph)_2Pt(SO_2)Pd(phen)B_{10}H_{10}$ compared to that in (**1**-Pt_2).[2]

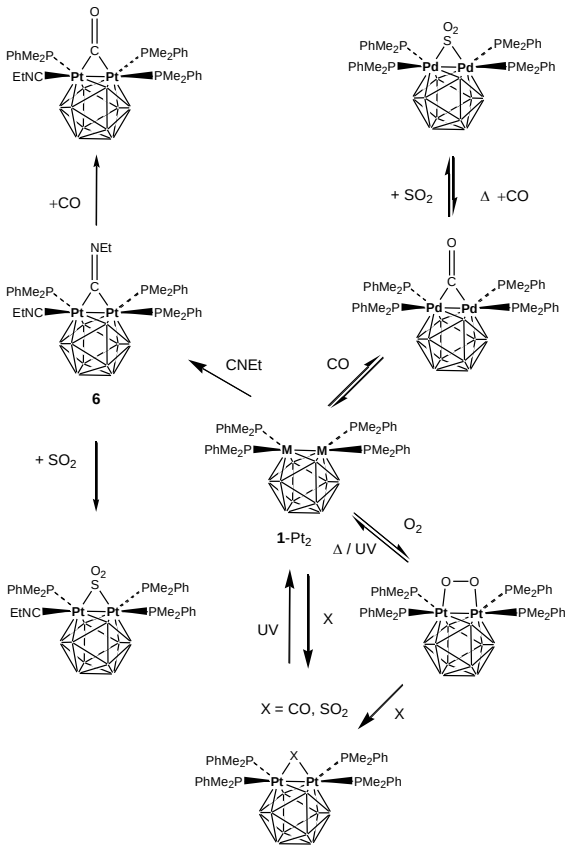

Scheme 1. Some examples of the quantitative reactions of the diplatinadodecaborane cluster compound, $L_4MM'B_{10}H_{10}$ with compound numbers for those discussed in the text.

In an interest to extend the set of small molecules that interact with the dimetallic borane cluster compound (**1**-Pt_2), we turned our attention to nitric oxide. NO is a free radical species, its unpaired electron distinguishing it from the other small molecule ligands, listed above, that are known to interact

with (**1**-Pt_2). Additionally, NO has been shown to be an important regulator and mediator of numerous processes in the nervous, immune, and cardiovascular systems. This has stimulated a general interest in the chemistry and biochemistry of NO[3] and derivatives such as metal nitrosyl complexes.[4] Also of interest are strategies to deliver NO to biological targets on demand.[5] One such strategy would be to employ a precursor which displays relatively low chemical reactivity but is photochemically active to release NO. This proposition led us to investigate whether dimetallic cluster (**1**-Pt_2) could take up NO to form a bridging metal nitrosyl-like interaction with the Pt-Pt vector of the cluster that would, say under UV irradiation, release the NO molecule on demand.

Results and discussion

A dichloromethane solution of $(PMe_2Ph)_4Pt_2B_{10}H_{10}$ (**1**-Pt_2)[1a, 1b] together with *ca.* four equivalents of nitric oxide was allowed to react overnight. The reaction was monitored periodically by NMR spectroscopy, which showed a number of mixed species forming with time. After leaving overnight, the phosphorus spectrum (Figure S1) showed a mixture of three species, including a strong peak for free dimethylphenylphosphine, with all other resonances attributed, after workup by thin-layer chromatography (TLC), to two products: red-brown $(PMe_2Ph)_8Pt_8B_{40}H_{40}$ (**2**-Pt_8) and grey-black $(PMe_2Ph)_5Pt_4B_{20}H_{20}$ (**3**-Pt_4) in yields of 38 % and 34 % respectively (Scheme 2).

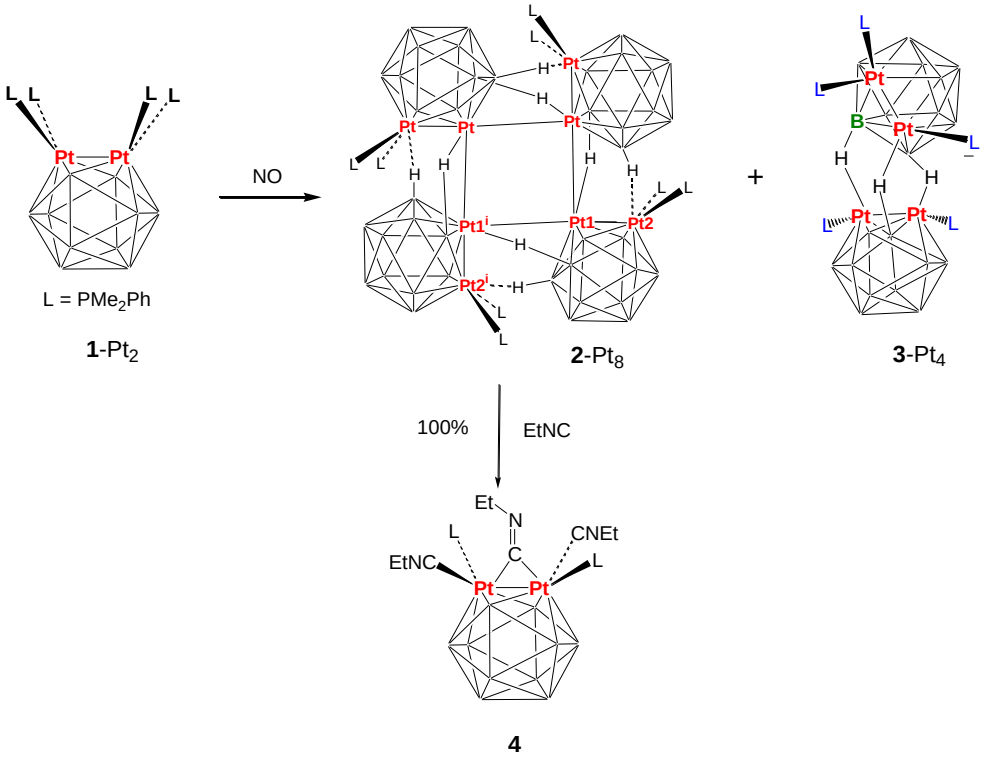

Scheme 2. *Endo*-polyhedral metallaborane cluster conglomerates (**2**-Pt_8) and (**3**-Pt_4) and subsequent reaction product **4**. Each cluster boron vertex holds an *exo*-terminal hydrogen atom although only *inter*cluster bridging hydrogen atoms are shown in order to aid clarity.

Table 1. ^{11}B, ^{1}H and ^{31}P NMR data for $[(PMe_2Ph)_4Pt_8B_{40}H_{40}]$ (**2**-Pt_8) at 291 K in CD_2Cl_2 solution.

Assignment	$\delta(^{11}B)$	$\delta(^{1}H)$[a]
	+18.9	+3.07
	+16.3(2)	+5.79(59),[b] +4.46
	+12.5(2)	+4.84, +1.11
	+10.4	+2.73
	+4.9	+3.94
	-9.4	+0.28(87) [b]
B8	-24.7	+2.11(58) [b]
B10	-28.0	+1.38(54) [b]
$^{13}C(^{1}H_3)$[c]		+20.2(+2.15), +16.6(+1.89)
		+20.9(+1.74), +13.6(+1.13)
δ (^{31}P)[d]	-10.2 (20, 2889)	
	-10.6 (20, 2623)	

a) See Figures S2 and S3.
b) Exhibits platinum satellites: $^{n}J(^{195}Pt\text{-}^{1}H)$/Hz in parentheses.
c) All resonances doublets: $^{2}J(^{1}H\text{-}^{31}P)$ *ca.* 10 Hz; $^{1}J(^{13}C\text{-}^{31}P)$ 33, 33, 34, 26 Hz respectively (Figure S4). Phenyl carbons +128 to +135 ppm.
d) $CDCl_3$ solution at 293 K. Doublets: $^{2}J(^{31}P\text{-}^{31}P)$ and $^{1}J(^{31}P\text{-}^{195}Pt)$/Hz, respectively, in parentheses (Figure S5).

The compounds were characterized by mass spectrometry, multielement NMR spectroscopy, and single-crystal X-ray diffraction studies. Boron-11, phosphorus-31, carbon-13, and proton NMR data (see Figures S1-S8 for spectra) are listed in Tables 1 and 3 for compounds (**2**-Pt_8) and (**3**-Pt_4) respectively, and selected interatomic distances and angles are listed in Table 2. The electrospray ionisation (ESI) mass spectra for the compounds, which display a good correspondence between the calculated and measured isotope envelopes and accurate masses, are shown in Figures S9 and S10 respectively. A drawing of the molecular structure of (**2**-Pt_8) is given in Figure 1a and the characterisation of this compound will be discussed first. The asymmetric unit, shown in Figure 1b, comprises a *closo*-diplatinadodecaborane $\{(PMe_2Ph)_2Pt_2B_{10}H_{10}\}$ cluster in which two phosphine ligands have been lost from one metal, Pt1. The molecule possesses a four-fold rotoinversion axis in the center of a 'butterfly' quadrilateral defined by the Pt1 cluster vertex.

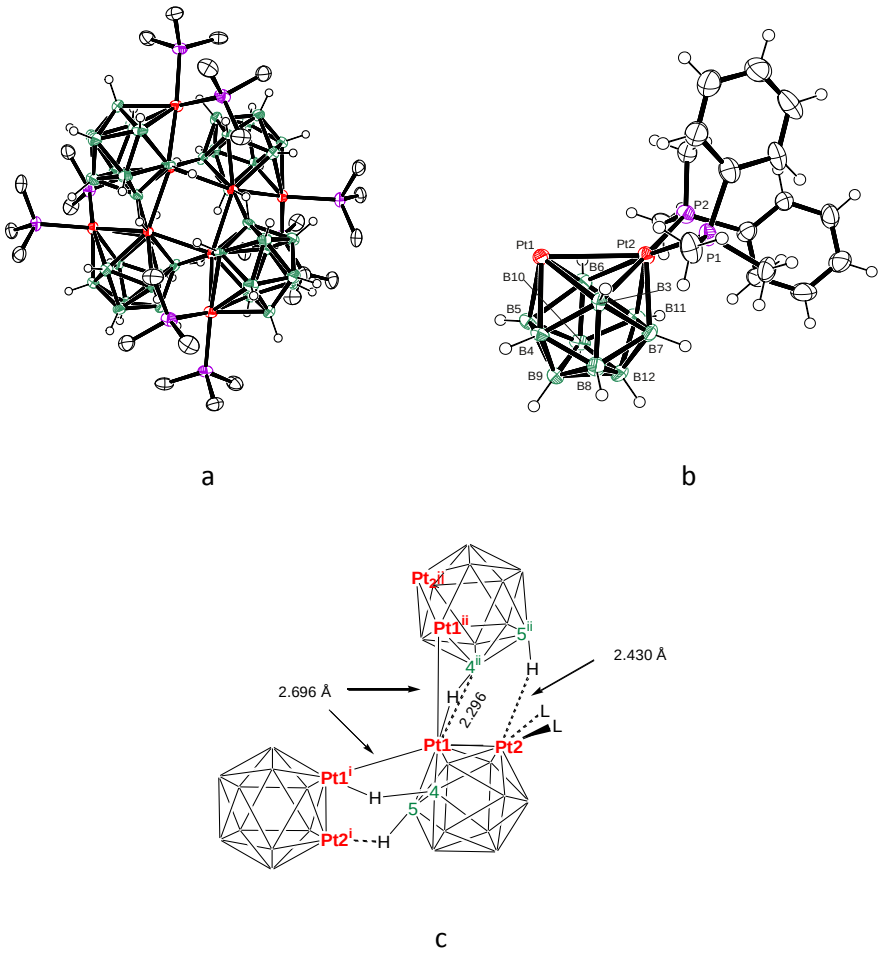

Figure 1. The molecular structure of $(PMe_2Ph)_8Pt_8B_{40}H_{40}$ (**2**-Pt_8) (a) with 50% probability ellipsoids for non-hydrogen atoms. Phenyl rings, except for the *ipso* carbon atoms, and the methyl hydrogen atoms are not shown in order to aid clarity. The molecule possesses a four-fold rotoinversion axis in the center of the quadrilateral defined by the Pt1 metal atoms. Vertex B4 in the asymmetric unit (b) holds the hydrogen atom bridging to $Pt1^i$ in the adjacent sub-cluster and B5 holds the hydrogen atom weakly interacting with $Pt2^i$ in an adjacent unit. Selected interatomic dimensions are listed in Table 2. (c) Schematic diagram of the intracluster bonding interactions.

Thus, the vacant coordination sites created by the loss of the phosphine ligands on the Pt1 vertex of each 12-vertex cluster unit are then filled by two modes of connection: one, bonding to symmetry-related adjacent clusters via Pt1-$Pt1^i$ and Pt1-$Pt1^{ii}$ metal-metal linkages with separations of 2.6962(4) Å and, second, a $Pt1^i$-μH4-B4 3-center, 2-electron bond to the adjacent cluster (see Figure 1c). The $Pt1^i$–B4 distance of 2.296(9) Å is well within the range of the other Pt-B intracluster distances [2.197(7) to 2.371(9) Å], suggesting a strong bonding interaction. If this were a two-center bond with no bridging hydrogen atom, the distance would be expected to be *ca.* 2.0 Å.[6] The bridging hydrogen atom was not

directly observed in the electron density map, although this is not unexpected due to its proximity to a third-row transition metal. The infrared spectrum shows a strong broad peak at 2490 cm^{-1} and no peak that can definitively be assigned to hydrogen bridging to platinum, although this is common for other reports on compounds with Pt-H-B or, for example, Pd-H-B bonds, in which no such peaks are mentioned.[7] However, selective decoupling of the boron resonances in the proton NMR spectrum of **2** clearly showed the presence of ten proton resonances attached to boron (Table 1, Figure S2). It is well recognised that X-ray determined distances to hydrogen atoms are unreliable, but their positions, located by XHYDEX[8] calculation, compare well to distances determined by neutron diffraction,[9] and we have previously had good success matching HYDEX calculated positions to those from X-ray diffraction and DFT calculation for third row transition metal terminal and bridging hydrides.[10] Thus, coordinates for the position of μH4 were inferred from an XHYDEX calculation using the initial X-ray diffraction data and then the new μH4 coordinates were inserted into the refinement with the same geometrical restraints and displacement parameter constraints as the rest of the cage hydrogens. This resulted in a satisfactory behaviour for the atom. In support, it may be noted that compound **3**-Pt_4 features three more strongly defined Pt-μH-B interactions, but these are discussed in detail later. The XHYDEX calculated distances are $Pt1^{i}$–H4 1.83 Å and B4-H4 1.28 Å. Another notable potentially weak interaction may occur between the second platinum vertex, Pt2, in the asymmetric unit and the terminal hydrogen atom, $H5^{i}$, on $B5^{i}$ of the adjacent cluster with a Pt-H separation of 2.42(6) Å, which is less than the 3.49 Å sum of the van der Waals radii (H 1.2 Å, Pt 2.29 Å).[11] This may contribute to the formation of the cluster conglomerate. There are a number of structurally characterised tetramers with either four *ortho*-dicarbadodeaboanyl and dodecaboranyl clusters linked only by isolated metal units, such as Hg,[12] Cu[13] or Ni,[13] but compound (**2**-Pt_8) holds closer similarities to the tetrapalladium carbaborane complex,[14] (**5**-Pd_4) shown in Schematic structure **I**, which also has a central Pd_4 butterfly core surrounded by four dicarbadodecaborane clusters. Here the large molecular size also results in very broad boron-11 NMR resonances. There is also an interaction between one *exo*-terminal hydrogen atom on each carbaborane cluster and one of the palladium atoms with a Pd–B distance of 2.92(1) Å. In this case, a single-crystal structural analysis apparently located the bridging hydrogen atom. It may be noted that we have supported the position of the bridging proton in this compound with an XHYDEX calculation giving a very low potential energy well at 1.33 Å from boron and 1.87 Å from palladium, and these are more realistic distances than those located by X-ray crystallography. Compound (**2**-Pt_8) is considerably more novel than (**5**-Pd_4), or the linked units mentioned above, in that the metal atoms forming the central quadrilateral are themselves cluster vertices rather than *exo*-terminal substituents, resulting in a more condensed metallaborane cluster conglomerate held together by multicentre bonding.

[Insert Schematic structure I here]

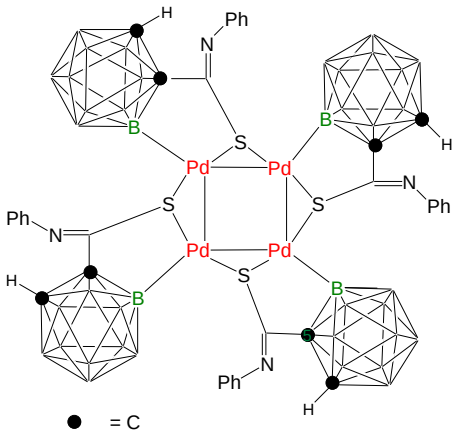

I (**5**-Pd_4)

Table 2. Selected interatomic distances (Å) and angles (°) for $(PMe_2Ph)_8Pt_8B_{40}H_{40}$, (**2**-$Pt_8$), and $(PMe_2Ph)_5Pt_4B_{20}H_{20}$, (**3**-$Pt_4$)**,** together with $(PMe_2Ph)_4Pt_2B_{10}H_{10}$, (**1**-$Pt_2$), for comparison.

Assignment	**1**	**2**	**3**- A	**3**-B
Pt1 - Pt2	2.9552(4)	2.8443(4)	2.8805(3)	2.7710(4)
Pt2 - P1	2.3344(4)	2.3824(19)	2.3268(15)	
Pt2 - P2	2.3382(4)	2.3604(17)	--	2.2985(17)[a]
Pt2 - B3	2.3626(17)	2.318(7)	2.234(8)	2.369(6)
Pt2 - B6	2.3101(18)	2.370(9)	2.303(8)	2.280(8)
Pt1 – P1			2.3387(15)	2.3109(17)
Pt2 - B7	2.2225(18)	2.219(8)		
Pt2 - B11	2.2035(18)	2.222(8)	2.199(7)	2.185(7)
Pt1 - B3	2.3101(18)	2.267(8)	2.317(7)	2.280(7)
Pt1 – B4	2.2035(18)	2.206(8)	2.234(8)	2.3109(17)
Pt1 - B5	2.2225(18)	2.198(7)	2.229(7)	2.186(7)
Pt1 – B6	2.3626(17)	2.210(8)	2.323(7)	2.283(8)
$Pt1^{i}$ - B4		2.296(9)		
$Pt1^{i}$ – B5		2.705(7)		
$Pt1^{i}$ – H4		1.89(9)		
Pt1 – $Pt1^{i}$		2.6962(4)		
$Pt2^{i}$ - H5		2.42(6)		
B4 – H4		1.06(4)		
Pt1-$Pt1^{i}$-$Pt1^{ii}$		88.478(4)		
P1-Pt2-P2		93.90(7)	96.52(6)	
P1–Pt2–Pt1		124.02(5)		

a) Distance to P3B

The boron NMR spectrum for compound (**2**-Pt_8) is shown together with that of (**1**-Pt_2) for comparison in Figure 2 illustrating the underlying similarity between (**1**-Pt_2) and (**2**-Pt_8). The peak width at half-maximum height (FWHM) in (**2**-Pt_8) for the high-field boron resonances at $\delta(^{11}B)$ -25 and -28 ppm are *ca*. 350-400 Hz compared to *ca*. 100 Hz for the equivalent resonance in (**1**-Pt_2), and are indicative of the large size of the molecule. This makes assignment of the resonances difficult as the boron and proton signals show no platinum satellites and the broadness of the resonances negates the effectiveness of 2D proton and boron COSY correlations.

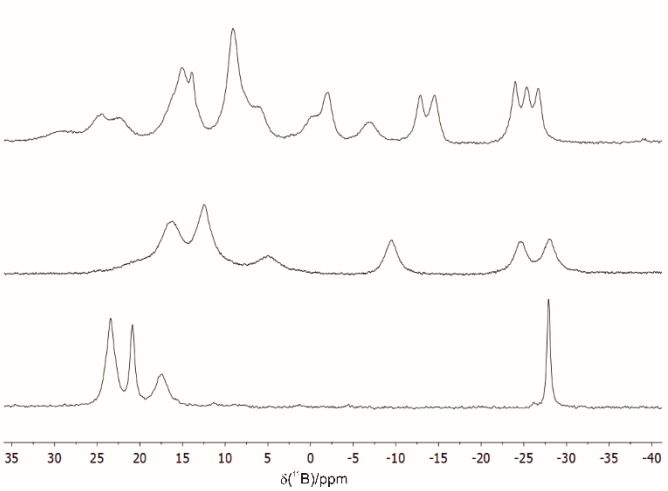

Figure 2. ^{11}B-{^1H} NMR spectra of $(PMe_2Ph)_5Pt_4B_{20}H_{20}$ (**3**-Pt_4, upper), $(PMe_2Ph)_8Pt_8B_{40}H_{40}$ (**2**-Pt_8, center) and $(PMe_2Ph)_4Pt_2B_{10}H_{10}$ (**1**-Pt_2, lower).

Although we have no direct information regarding the reaction mechanism leading to the products, it is notable that the reaction of (**1**-Pt_2) with NO is blocked by having a CO across the Pt-Pt vector in $(PMe_2Ph)_4(CO)Pt_2B_{10}H_{10}$, even after leaving overnight at 70 °C, suggesting that NO initially interacts across the metal-metal vector. Phosphine ligand displacement from (**1**-Pt_2) by an incoming ligand, EtNC, has been observed previously to afford $(EtNC)_2(PMe_2Ph)_3Pt_2B_{10}H_{10}$,[15] (**6**, see scheme 1) although cluster conglomeration presumably does not occur here as the PMe_2Ph is immediately replaced by the isonitrile ligands (see also compound **4** below).[1d]

An alternative route to these multimetallic metallaboranes conglomerates is suggested from the synthesis of the tetranuclear compound (**5**-Pd_4) mentioned above, which was synthesised from the *ortho*-dicarbadodecaborane anion and $PdCl_2(MeCN)_2$, in which the nitrile ligands are easily displaced. The mixed metal bimetalladodecaborane cluster compounds $(PMe_2Ph)_4MM'B_{10}H_{10}$ described here are synthesised from the reaction of $[(PMe_2Ph)_2PtB_{10}H_{10}]^{2-}$ and $PtCl_2(PMe_2Ph)_2$, thereby suggesting that

further mixed bimetallic conglomerates could be synthesised directly using, for example, $PdCl_2(MeCN)_2$ or $[BF_4]_2[M(MeCN)_x]$, (M = Pd, Co, Ni, Fe etc).[16] We are currently investigating this possibility.

The molecular structure of the second compound isolated in 34% yield from the reaction, $(PMe_2Ph)_5Pt_4B_{20}H_{20}$, (**3**-$Pt_4$), is shown in Figure 3 and selected interatomic dimensions are given in Table 2.

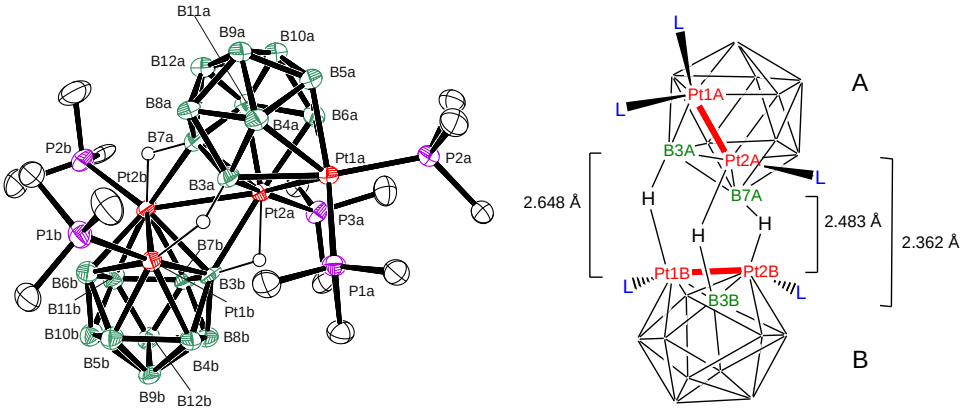

Figure 3. (Left) The molecular structure of $(PMe_2Ph)_5Pt_4B_{20}H_{20}$ (1.5 C_6H_6), (**3**-Pt_4), with 50% probability ellipsoids for non-hydrogen atoms. Cage hydrogen atoms, except for bridging hydrogen atoms, benzene solvent molecules, methyl hydrogen atoms and phenyl groups except for *ipso* carbon atoms are not shown to aid clarity. (Right) Schematic structure of (**3**-Pt_4) illustrating interatomic distances.

NMR data are listed in Table 3 and are fully in accord with the crystallographic data. The integrated ^{11}B-{^1H} NMR spectrum indicates an unsymmetrical compound with 20 boron resonances (Figure 2). The ^{31}P-{^1H} spectrum features five different singlet resonances each with ^{195}Pt satellites (Figure S1 inset). The proton NMR spectrum shows ten different methyl resonances, and ^1H-{^1B(selective)} experiments show signals due to twenty *exo*-terminal protons (Figure S6). Again, as with (**2**-Pt_8), the overall broadness of the proton resonances and the tendency of the platinum bridging protons to appear amongst the terminal B-H_{exo} resonances rather than at higher field, as commonly seen in similar platinaborane[17] and platinacarboranes,[7b] results in the ^{195}Pt-$^1H_{bridge}$ satellites overlapping with the other B-H_{exo} peaks. The exception is the resonance at $\delta(^1H)$ +0.65 ppm with $J(^{195}Pt$-$^1H)$ 588 Hz, and this is probably due to the proton bridging Pt2a-B3b, as this is the shortest intercluster separation at 2.360(7) Å, thus implying a shorter distance and a stronger Pt-μH coupling. The chemical shift of the bridging hydrogen atom together with the size of the coupling constant may be used as a metric for the strength of the Pt-H interaction. With full hydridic character to the terminal Pt-H bond one might expect, for example, a chemical shift of *ca.* -10 ppm,[7c] whereas Pt-μH-B three-center bonds commonly appear to lower field at *ca.* $\delta(^1H)$ -5 to -6 ppm.[6a, 7a, 7c, 18] In contrast to compound (**2**-Pt_8), electron density for all three bridging

hydrogen atoms was observed in the X-ray data and their positions were also confirmed by XHYDEX calculation with the Pt-H and B-H distances all *ca.* 1.67 and 1.25 Å respectively. The B-μH→Pt interaction could be viewed as acting as an electron-donating ligand, subrogating the lost phosphine. The P1a-Pt1a-P2a angle of 96.52(6)° compared to the P-Pt-(PtμHB centroid) angles of *ca.* 92° are sufficiently close to suggest that the bridging hydrogen atoms are essentially replacing the expelled phosphine ligands.

Table 3. ^{11}B, ^{1}H and ^{31}P[a] NMR data for $(PMe_2Ph)_5Pt_4B_{20}H_{20}$, (**3**-$Pt_4$), in $CDCl_3$ solution at 291 K.

Assignment	δ(^{11}B)/ppm	δ(^{1}H)/ppm	
B9B	+28.6	+3.06	
	+24.5	+4.20	
	+22.2	+4.77	
	+14.9(2)	+5.1,+2.87	
	+13.9	+4.67	
	+9.0(4)	+4.24(2), +4.19(2)	
	+7.7	+3.66	
	+6.0	+3.21	
	-0.3	+2.25	
B3B	-2.0	+0.65[b]	
	-7.2	+2.19	
	-12.9	+1.97	
B10B	-14.6	+2.21	
B10a	-24.0	+2.26	
B8a	-25.4	+2.24	
B8B	-26.8	+2.38	
Me: $^{13}C(^{1}H)$ /ppm[c]	^{3}J(^{1}H-^{195}Pt)/Hz	δ(^{31}P)/ppm	^{2}J(^{195}Pt-^{31}P)/Hz
+21.1(+2.32), +18.2(+2.26)	10	-6.69	2750
+15.3(+2.02), +15.3(+1.78)	8	+2.94	2945
+16.3(+1.91), +19.7(+1.85)	10	+0.16	2920
+17.3(+1.53), +17.3(+1.52)	[d]	+10.89	3119
+17.7(+1.07), +15.3(+0.94)	9	+5.35	3074

a) Measured at 223 K (Figure S1). b) Exhibits platinum satellites $^{n}J(^{195}Pt-^{1}H)$ 588 Hz. c) See Figure S5. d) Obscured by solvent resonances.

The two compounds here are formed by the loss of phosphine ligands from **1**-Pt_2 with the coordination site vacancies thus created allowing the condensation of four or two molecules to form products **2**-Pt_8 and **3**-Pt_4. Though metal ligands are not directly included in skeletal electron counting formalisms,[19] the loss of the donor electron pairs from the phosphines suggests that the reaction can be regarded as an oxidative coupling of the clusters. If **1**-Pt_2 is regarded as a classical *closo*-

bimetalladodecahedral cluster with 2*n*+2 skeletal bonding electrons according to electron-counting rules,[19-20] then the two {$(PMe_2Ph)_2Pt$} moieties in **1**-Pt_2 would be required to be octahedral 18-electron Pt(IV) centers with a Pt-Pt bond between them. However, the {$(PMe_2Ph)_2Pt$} moieties are better regarded as 16-electron Pt(II) species as the intermetal distance of 2.96 Å suggests a very weak, essentially non-bonding, interaction and the platinum atoms, in their propensity to take up appropriate electron donating bridging groups retain the property of square-planar d^8 group 10 transition metals.[15] Thus, the non-bonding Pt-Pt vector closes up to a distance appropriate for a Pt-Pt bond of *ca.* 2.7 to 2.8 Å when bridged by O_2, CO and SO_2 (Pt covalent radius 1.36 Å[21]).

Within the compounds **2**-Pt_8 and **3**-Pt_4, one of the most notable features in terms of electron counting is the sharing of the electrons, in what would be a terminal B-H_{exo} cluster hydrogen atom in the single cluster precursor, which are now inter-subcluster hydrogen bridges. Thus each adjacent subcluster shares two electrons with its neighbor. The Pt1 – $Pt1^i$ distance of 2.6962(4) Å in the central platinum core suggests four strong 2-center, 2-electron bonds whereas the Pt1-Pt2 distance of 2.8443(4) Å, while 0.12 Å shorter than that in the single cluster precursor, is also 0.12 Å longer than the sum of the covalent radii and is therefore not fully 'closed' suggesting that **2**-Pt_8 might be able to sequester ligands similarly to **1**-Pt_2 (see later).

There are a number of hydrogen-bridged-conjoined binary monometalla-cluster compounds with metal-metal linkages in the Cambridge Structural Database (CSD)[22] and with a hydrogen bridged M-B distance of < 2.6 Å,[23] although only two, as far as we are aware, contain platinum: one, [6',10-(μ-H)-10-PEt_3-*closo*-10,1-$PtCB_8H_8]_2$ (Schematic structures **II**)[7b] in which the two clusters are held together by two M-μH-M bridges with similar Pt – B separations and an intermetal distance of 2.73 Å,

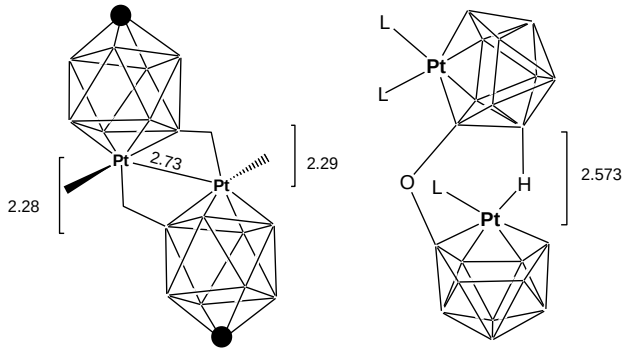

II **III**

and, second, [{7,7-$(PMe_2Ph)_2$-7-$PtB_{10}H_{10}$-μ-8,8'-O-μ-4,7'-H-{7'-PMe_2Ph)-7'-$PtB_{10}H_{11}$}] (schematic structure **III**), in which there is one B-μH-Pt interaction between two clusters and where the 2-electron bridging linkage subrogates the electron pair donor molecule PMe_2Ph in a *nido*-platinaundecaborane cluster. Here it is notable that there is no consequent overall change in the structures of the *nido*-

metallaundecaborane clusters.[24] The three XHYDEX calculated Pt – H and B – H distances in both of these compounds of 1.78 and 1.33 Å respectively are the same, and are also similar to those in (**2**-Pt_8), but slightly longer than those in the triply bridged **3**-Pt_4. The consistency in H-atom locations suggests that XHYDEX is working appropriately in this system.

In **2**-Pt_8, the Pt2 vertex retains two phosphine units and may keep some of the d^8 Pt(II) square-planar character whereas the Pt1 vertex, with the 2-center, 2-electron Pt-Pt bond together with electrons associated with cluster skeletal electron bonding may be regarded as a Pt(III) or Pt(IV) center. Such a mixed valence description has been applied to the platinacarbaborane (schematic **II**). However, such precise distinctions in oxidation states based on classical coordination compound theory might be inappropriate in this large molecule which could be better regarded as a delocalised aggregate.

As mentioned above, the Pt1-Pt2 distance of 2.8443(4) in **2** being midway between that in **1** and that in the deoxygenated or carbonylated species for **1** led us to infer that the sequestering ability of (**2**-Pt_8) would still be intact to some degree, although weaker than in **1**. This is borne out by the observation that the compound is clearly air stable and does not take up dioxygen, unlike the single-cluster compound (**1**-Pt_2). Thus an attempt to re-form (**1**-Pt_2) by the addition of the PMe_2Ph ligand was unsuccessful – even after overnight heating at 70 ° C. Also, a dichloromethane solution of **2** under a CO atmosphere was unchanged. However, the addition of excess EtNC to a solution of (**2**-Pt_8) in $CDCl_3$ in an NMR tube afforded [1,2-$(EtNC)_2$-μ(1,2-EtNC)-1,2-$(PMe_2Ph)_2$-1,2-$Pt_2B_{10}H_{10}$] (**4**) quantitatively (Eqn. 1). Phosphorus, boron and proton NMR spectroscopy of the reaction mixture showed one product with no other boron-containing compounds, and the isolated product was characterized by NMR spectroscopy, high resolution mass spectrometry (Figure S11), and a single-crystal X-ray diffraction study. NMR data are listed in the experimental section and Figure 4 shows a drawing of the molecular structure together with selected interatomic dimensions.

$$(PMe_2Ph)_8Pt_8B_{40}H_{40} + 12\ EtNC \rightarrow 4\ [(EtNC)_3(PMe_2Ph)_2Pt_2B_{10}H_{10}] \qquad \text{---- (1)}$$

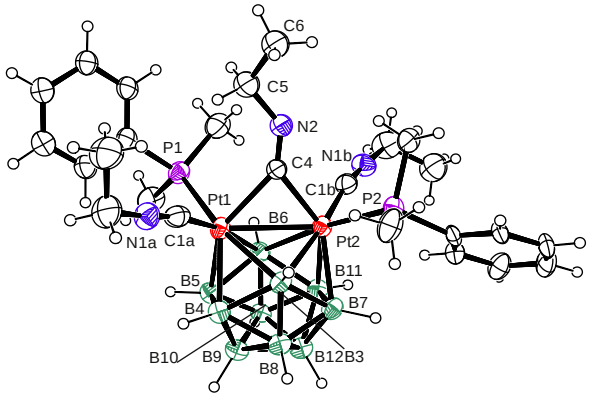

Figure 4. ORTEP-3 drawing of the molecular structure of one of the two molecules in the asymmetric unit of [1,2-$(EtNC)_2$-μ(1,2-EtNC)-1,2-$(PMe_2Ph)_2$-1,2-$Pt_2B_{10}H_{10}$].8$CDCl_3$ **4** with 50% probability ellipsoids for non-hydrogen atoms. $CDCl_3$ solvent molecules are not shown to aid clarity. Selected interatomic distances (Å) and angles: (°) to Pt1: Pt2 2.717(7), C1a 2.002(14), C1b 2.000(18), C4 2.21(3), P1 2.336(5), P2 2.320(5), B3 2.317(12), B4 2.236(13), B5 2.235(13), B6 2.258(12). To Pt2: C1b 2.000(18), C4 2.15(3), P2 2.320(5). Also: C4 – N2 1.18(3), C1a – N1a 1.149(16), C1b – N1b 1.149(19). Angles (°): P1-Pt1-C1a 97.0(5), P1-Pt1-Pt2 113.0(2), P1-Pt1-C1a 90.1(7), Pt1-C4-Pt2 77.1(9).

The boron NMR spectrum, which shows four resonances in a 2:2:4:2 relative intensity pattern between +14.5 and -17.7 ppm, resembles that for the known compound $(EtNC)_2(PMe_2Ph)_3Pt_2B_{10}H_{10}$, **6**, mentioned earlier (see scheme 1) which has a similar, although asymmetric, pattern between +15.3 and -16.2 ppm.[1d] Selective decoupling of the boron resonances shows ten terminal boron hydrogen atoms (Figure S8). Full NMR for **4** data are listed in the Experimental section. The data collected from the single-crystal X-ray structural study were hampered by the small crystal size, the significant decomposition of the crystal in the X-ray beam, together with disorder in the bridging isonitrile group, but the derived structure is fully consistent with the NMR and mass spectrometric data. Interatomic distances such as the Pt–Pt and those associated with the terminal and bridging isonitriles are not significantly different from those of compound **6**. It may be noted that now in **4** both platinum atoms hold a phosphine ligand, thus indicating that a phosphine migration has occurred. As seen in the synthesis of **6** from the addition of isonitrile to **1**-Pt_2, the isonitrile is able to replace PMe_2Ph and thus, in the case of the reaction of **2**-Pt_8, it may induce a concerted migration of the phosphine rather than disassociation and re-addition of PMe_2Ph, as **2**-Pt_8 is inert to the simple addition of phosphine. This may occur by initial attack on Pt2, which holds two phosphine ligands, is less sterically hindered than Pt1, and retains, as discussed earlier, more 16-electron square-planar character than Pt1. Also similarly to **6**, which undergoes a further quantitative reaction with CO to form $(EtNC)(CO)(PMe_2Ph)_3Pt_2B_{10}H_{10}$, compound **4** reacts with CO. However, we have not yet fully characterised the product from this reaction. The demonstrated displacement of the phosphine by isonitrile clearly suggests that NO may behave similarly and therefore affords insight into the mechanism of the formation of **2**-Pt_8 and **3**-Pt_4.

Conclusion

This contribution presents the unusual interaction between the $(PMe_2Ph)_4Pt_2B_{10}H_{10}$ (**1**-Pt_2) cluster system, known for its ability to sequester gases, and nitric oxide, thus adding to the portfolio of interesting interactions of $(PMe_2Ph)_4MM'B_{10}H_{10}$ species with small molecules. The anticipation was for the formation of a bridging metal nitrosyl-like interaction with the Pt-Pt vector in the **1**-Pt_2 cluster that would, say under UV irradiation, release the NO molecule on demand. Instead we observe the unpredicted and

unprecedented NO-triggered fusion of multiple metallaborane clusters and the formation of 2- and 4-membered conglomerates, **2**-Pt_8 and **3**-Pt_4, that are structural curiosities from the perspective of both cluster borane and cluster platinum chemistries.

An interesting final consideration, raised by a reviewer, regards the spin multiplicity of the sequestered ligands. So far, this system reveals that O_2 (triplet groundstate, S=1), SO_2 and CO (singlet groundstates, S=0) molecules simply reversibly "bind" to the Pt-Pt edge in the $(PMe_2Ph)_4Pt_2B_{10}H_{10}$ (**1**-Pt_2) cluster, but the NO(·) radical (doublet groundstate S=1/2) changes the entire reaction, fusing platinaborane clusters and forming further Pt-Pt bonds. Whether it is the electronic states of these ligands that play the key role in the reaction mechanisms is the subject of our ongoing investigation into the $(PMe_2Ph)_4MM'B_{10}H_{10}$ system.[25]

Experimental section

General. Reactions were carried out under an argon atmosphere using standard Schlenk-line techniques. $(PMe_2Ph)_2Pt_2B_{10}H_{10}$ (**1**-Pt_2) was prepared according to the literature method by refluxing $(PMe_2Ph)_2PtB_{10}H_{12}$ with PMe_2Ph, and $(PMe_2Ph)_4(O_2)Pt_2B_{10}H_{10}$ was crystallised from aerated hexane/CH_2Cl_2 solutions of **1**-Pt_2 at -35 °C.[1b] Nitric oxide was isolated from a reaction to prepare $FeCl_2(MeCN)_2$ from $NOBF_4$ and Fe[16] and stored in a glass bulb over P_2O_5. Preparative thin-layer chromatography (TLC) was carried out using 1 mm layers of silica gel G (MN Silica Gel G/UV254) made from water slurries on glass plates of dimensions 20 × 20 cm and dried in air at 80 °C. IR spectra were recorded at resolution 4 cm^{-1} on a Nicolet Nexus 670 spectrometer equipped with liquid nitrogen-cooled MCT detector and a ZnSe ATR crystal. NMR spectra were recorded on a JEOL 600 MHz (14.1 T) spectrometer, using ^{11}B, ^{11}B-{^1H} ^1H, ^1H-{^{11}B(broadband)}, ^1H-{^{11}B(selective)} and HMQC (Heteronuclear Multiple-Quantum Correlation) techniques. ^1H NMR chemical shifts, $\delta(^1H)$, were measured relative to partially deuterated solvent peaks but are reported in ppm relative to tetramethylsilane. ^{11}B chemical shifts $\delta(^{11}B)$ are quoted relative to $[BF_3(OEt)_2)]$ in $CDCl_3$ and ^{31}P chemical shifts $\delta(^{31}P)$ are quoted relative to 85% aqueous H_3PO_4. Mass spectra were measured using LTQ Orbitrap XL hybrid mass spectrometer (Thermo Fisher Scientific, Waltham, MA, USA) equipped with an electrospray ion source. The mobile phase was acetonitrile flowing at 100 μL/min. The sample was dissolved in chloroform/acetonitrile and injected into the mobile phase using a 5-μL loop. Spray voltage, capillary voltage, tube lens voltage, and capillary temperature were 5.0 kV, 9 V, 150 V, and 275 °C, respectively. The Orbitrap mass spectra were recorded at the resolution of 100,000.

Syntheses

$(PMe_2Ph)_8Pt_8B_{40}H_{40}$, 2-$Pt_8$ and **$(PMe_2Ph)_5Pt_4B_{20}H_{20}$, 3**-$Pt_4$. On a Schlenk line, CD_2Cl_2 was condensed into an NMR tube holding a Teflon screw cap and containing $(PMe_2Ph)_4Pt_2B_{10}H_{10}$ (17 mg, 16 μmol). A measured volume of nitric oxide amounting to *ca.* 22 μmol was condensed into the tube which was then sealed and allowed to warm to room temperature, then shaken and left overnight. ^{11}B NMR showed a mixture of new resonance peaks over time suggesting a number of intermediate species. ^{31}P NMR the next day (Figure S1) showed free PMe_2Ph and resonances which were later attributed to the compounds (**2**-Pt_8) and **3**-Pt_4 below. The reaction mixture was washed through a filter frit with CH_2Cl_2, the filtrate reduced in volume, applied to a preparative TLC plate and developed in CD_2Cl_2/hexane. Two main bands were evident: A, brown/red, R_F 0.75 and B, gray R_F 0.5. The bands were removed from the silica gel with CH_2Cl_2. NMR spectroscopy showed one species with no minor impurities for band A, identified as $(PMe_2Ph)_8Pt_8B_{40}H_{40}$ (**2**-Pt_8, 4.6 mg, 1.5 μmol, 38 % yield based on $(PMe_2Ph)_2Pt_2B_{10}H_{10}$). Single crystals were obtained by hexane diffusion through a layer of benzene into a $CDCl_3$ solution of the compound. Band B was identified similarly as $(PMe_2Ph)_5Pt_4B_{20}H_{20}$ (**3**-Pt_4, 3.6 mg, 2.7 μmol, 34%). Single -crystals were obtained by pentane diffusion through a layer of benzene into a CD_2Cl_2 solution of the compound. Other very faint bands were apparent on the plate but they decomposed on attempts to crystallise them before carrying out NMR characterisation. Mass spectra for the sodium adduct of (**2**-Pt_8): Calc. for $C_{64}H_{128}B_{40}NaP_8Pt_8^+$ 3167.87133, Meas. 3167.87356 (+0.7 ppm, Figure S9). For (**3**-Pt_4): Calc. for $C_{40}H_{75}B_{20}NaP_5Pt_4^+$ 1733.49011, Meas. 1733.49241 (+1.3 ppm, Figure S10). IR ν_{max}(BH)/cm^{-1}, Figure S12): 2490 (**2**-Pt_8,) and 2488 (**3**-Pt_4). In a separate reaction CH_2Cl_2 (*ca*. 0.2 ml) was condensed into an NMR tube containing $(PMe_2Ph)_4(O_2)Pt_2B_{10}H_{10}$ (20 mg, 18 μmol) and six equivalents of NO was condensed in, the mixture allowed warm to ambient temperature, and left overnight. TLC as above next morning gave (**2**-Pt_8) (3.4 mg, 1.1 μmol, 27%), together with a purple boron-containing band, 1.1 mg, which decomposed during crystallisation attempts.

$(EtNC)_3(PMe_2Ph)_2Pt_2B_{10}H_{10}$ 4. On the Schlenk line, $CDCl_3$ (*ca*. 0.2 ml) was condensed into an NMR tube containing $(PMe_2Ph)_8Pt_8B_{40}H_{40}$ (**2**-Pt_8, 3.6 mg) and excess EtCN was condensed into the tube (*ca.* 60 μmol) and left to react overnight during which time it went from the reddish color of (**2**-Pt_8) to pale yellow. The next day, NMR spectroscopy showed a quantitative conversion to [1,2-$(EtNC)_2$-μ(1,2-EtNC)-1,2-$(PMe_2Ph)_2$-1,2-$Pt_2B_{10}H_{10}$] **4**. Solvents and EtNC were then pumped off on the Schlenk line and $CDCl_3$ reintroduced. Following full NMR characterisation, single crystals were grown by condensing a small layer of benzene and then a larger layer of pentane into the NMR tube and storing at -35 °C. It may be noted that in addition to yellow crystals of the title compound, red insoluble crystalline 'blobs' also appeared over time. This was consistent in subsequent preparations. NMR data (293K, $CDCl_3$, see Figure S8): δ(^{11}B) [$^1H_{exo}$(intensities in parentheses)]/ppm: 2B +14.5[+5.45(2)], 2B +2.7[+1.1(2)], 4B

+0.3[+3.62(4)], 2B -17.7[+2.62(2), satellites, $^{n}J(^{195}Pt\text{-}^{1}H)$ 46 Hz]. δ(^{1}H) CH_3CH$_2$NC +1.17(9) [triplet, $^{2}J(^{1}H\text{-}^{1}H)$ 9 Hz]; MeCH_2NC +3.41(6)[broad] 5.7 Hz]; P(CH_3): +1.83(12) [doublet $^{2}J(^{31}P\text{-}^{1}H)$ 28 Hz, $^{3}J(^{195}Pt\text{ -}^{1}H)$ 22 Hz]. δ (^{31}P)/ppm -20.4 $^{1}J(^{195}P\text{ -}^{31}P)$ 2658 Hz. $^{1}J(^{195}Pt\text{-}^{195}Pt)$ 92 Hz (CD_2Cl_2, 223 K). HRMS Calc. for $C_{25}H_{47}N_3B_{10}P_2Pt_2^+$ 951.34658, Meas. 951.34418 (-2.5 ppm, Figure S11).

X-ray crystallography

Crystal data, data collection, and refinement information are given in Table 4 for compounds (**2**-Pt_8), (**3**-Pt_4) and **4**. A full description of the data collection and refinement may be seen in the Supporting Information.

Table 4. X-ray crystallographic information for compounds **2**, **3** and **4**.

Compound	**2**	**3**	**4**
CCDC	1978278	1978276	1978277
Chem form	$C_{64}H_{128}B_{40}P_8Pt_8$	$C_{40}H_{75}B_{20}P_5Pt_4 \cdot 1.5C_6H_6$	$C_{50}H_{94}B_{20}N_6P_4Pt_4 \cdot 8CHCl_3$
M_r	3138.5	1824.6	2854.8
Cryst syst	Tetragonal	Triclinic	Triclinic
Space group	*P*4/*n*	$P\bar{1}$	$P\bar{1}$
a (Å)	21.8818(3)	13.5302(4)	10.6353(2)
b (Å)	21.8818(3)	14.2930(4)	21.8941(5)
c (Å)	11.4152(3)	18.3556(5)	22.5326(4)
α (deg)	90	73.010(2)	92.712(2)
β (deg)	90	74.807(2)	94.663(2)
γ (deg)	90	69.260(3)	91.380(2)
V (Å^3)	5465.7(2)	3124.51(17)	5221.44(18)
Z	2	2	2
Reflns measd	40986	44540	78567
Unique reflns	4840	11062	20303
R_{int}	0.0793	0.0488	0.0917
R (on *F*, $F^2>2\sigma$)	0.0317	0.0314	0.0789[a]
R_w (on F^2, all data)	0.0740	0.0763	0.1908
GoF (on F^2)	1.057	1.063	1.692[b]
Refined params	305	825	513
Diff map min,max (e Å^{-3})	1.23, −1.02	2.25, −0.99	3.73, −3.22

[a] The observability threshold for **4** was 3σ (default for program Jana2006).[26]

[b] Jana2006 does not optimise the weighting scheme and uses weights as supplied direct from the experiment. Therefore, GoF is larger than from SHELX

ASSOCIATED CONTENT

Supporting Information

Selected NMR spectra for compounds (**2**-Pt_8), (**3**-Pt_4) and (**4**). Crystal data and structure refinement experimental details for (**2**-Pt_8), (**3**-Pt_4) and (**4**).

AUTHOR INFORMATION

Corresponding Author

Dr. Jonathan Bould E-mail: jbould@gmail.com

Author Contributions

The manuscript was written through contributions of all authors. All authors have given approval to the final version of the manuscript.

Notes

The authors declare no competing financial interests.

Acknowledgements.

We gratefully acknowledge the support of the Czech Science Foundation (Project No. 18-20286S) and the working group Interactions of Inorganic Clusters, Cages, and Containers with Light within the AV21 Strategy, Czech Academy of Sciences. Crystallographic data for compound **4** were supported by the project 18-10504S of the Czech Science Foundation using instruments of the ASTRA laboratory established within the Operational Program Prague Competitiveness - project CZ.2.16/3.1.00/24510.

References

1. (a) Bould, J.; McInnes, Y. M.; Carr, M. J.; Kennedy, J. D. Metallaborane reaction chemistry. A facile and reversible dioxygen capture by a B-frame-supported bimetallic: structure of $(PMe_2Ph)_4(O_2)Pt_2B_{10}H_{10}$. *Chem. Commun.* **2004,** (21), 2380-2381 DOI: 10.1039/b406974a; (b) Bould, J.; Kilner, C. A.; Kennedy, J. D. The capture of dioxygen, carbon monoxide and sulfur dioxide by $(PMe_2Ph)_4Pt_2B_{10}H_{10}$. *Dalton Trans.* **2005,** (9), 1574-1582 DOI: 10.1039/b419243e; (c) Bould, J.; Base, T.; Londesborough, M. G. S.; Oro, L. A.; Macías, R.; Kennedy, J. D.; Kubat, P.; Fuciman, M.; Polivka, T.; Lang, K. Reversible Capture of Small Molecules On Bimetallaborane Clusters: Synthesis, Structural Characterization, and Photophysical Aspects. *Inorg. Chem.* **2011,** 50 (16), 7511-7523 DOI: 10.1021/ic200374k; (d) Bould, J.; Londesborough, M. G. S.; Kennedy, J. D.; Macías, R.; Winter, R. E. K.; Císařová, I.; Kubat, P.; Lang, K. Isonitrile ligand effects on small-molecule-sequestering in bimetalladodecaborane clusters. *J. Organomet. Chem.* **2013,** 747, 76-84 DOI: 10.1016/j.jorganchem.2013.02.010.

2. (a) Bould, J.; Kennedy, J. D. Metallaborane reaction chemistry. A predicted and found tailored facile and reversible capture of SO_2 by a B-frame-supported bimetallic: structures of $(PMe_2Ph)_2PtPd(phen)B_{10}H_{10}$ and $(PMe_2Ph)_2Pt(SO_2)Pd(phen)B_{10}H_{10}$. *Chem. Commun.* **2008,** (21), 2447-2449 DOI: 10.1039/b800984h; (b) Bould, J.; Bown, M.; Coldicott, R. J.; Ditzel, E. J.; Greenwood, N. N.; Macpherson, I.; MacKinnon, P.; Thornton-Pett, M.; Kennedy, J. D. Metallaborane reaction chemistry. Part 12. Some interactions of acetylenes and isocyanides with selected metallaboranes. *J. Organomet. Chem.* **2005,** 690 (11), 2701-2720 DOI: 10.1016/j.jorganchem.2005.02.028.

3. Habib, S.; Ali, A. Biochemistry of Nitric Oxide. *Indian J. Clin. Biochem.* **2011,** 26 (1), 3-17 DOI: 10.1007/s12291-011-0108-4.

4. Hayton, T. W.; Legzdins, P.; Sharp, W. B. Coordination and Organometallic Chemistry of Metal−NO Complexes. *Chem .Rev.* **2002,** 102 (4), 935-992 DOI: 10.1021/cr000074t.

5. (a) Yamamoto, T.; Bing, R. J. Nitric Oxide Donors (44565). *Proceedings of the Society for Experimental Biology and Medicine* **2000,** 225 (3), 200-206 DOI: 10.1177/153537020022500306; (b) Rajasekharan-Nair, R.; Darby, L.; Reglinski, J.; Spicer, M. D.; Kennedy, A. R. Nitric oxide species as oxidising agents and adducts for soft scorpionates. *Inorg. Chem. Commun.* **2014,** 41, 11-13 DOI: https://doi.org/10.1016/j.inoche.2013.12.007.

6. (a) Ellis, D. D.; Jelliss, P. A.; Stone, F. G. A. Synthesis of rhenium–platinum complexes bearing carbaborane ligands and their unusual dynamic behavior. *J. Chem. Soc., Dalton Trans.* **2000**, 2113-2122 DOI: 10.1039/b002043p; (b) Lu, X. L.; McGrath, T. D.; Stone, F. G. A. Synthesis of the manganese-

monocarbollide dianion [1-NHBut-2,2,2-$(CO)_3$-*closo*-2,1-$MnCB_{10}H_{10}]^{2-}$: Reactions with transition metal cations. *Inorg. Chim. Acta* **2006,** 359 (9), 2665-2673 DOI: https://doi.org/10.1016/j.ica.2005.10.022.

7. (a) Goldberg, J. E.; Howard, J. A. K.; Müller, H.; Pilotti, M. U.; Stone, F. G. A. Synthesis and crystal structures of the complexes [RhPt(μ-H)(μ-CO)$(PEt_3)_2(PPh_3)(\eta^5$-$C_2B_9H_{11})$] and [RhPt{σ-C$(C_6H_4$Me-4)=C$(C_6H_4$Me-4)H}(CO)$(PEt_3)_2(PPh_3)(\eta^5$-$C_2B_9H_{11})$]. *J. Chem. Soc., Dalton Trans.* **1990,** (10), 3055-3061 DOI: 10.1039/dt9900003055; (b) Franken, A.; McGrath, T. D.; Stone, F. G. A. Two Metal−Monocarbollide Relatives of the $\{B_{20}H_{18}\}$ Double-Cluster Boranes. *Organometallics* **2010,** 29 (21), 4790-4792 DOI: 10.1021/om100471n; (c) Devore, D. D.; Howard, J. A. K.; Jeffery, J. C.; Pilotti, M. U.; Stone, F. G. A. Chemistry of polynuclear metal complexes with bridging carbene or carbyne ligands. Part 84. Carbaborane tungsten–platinum complexes having a μ-$CC_6H_3Me_2$-2,6 ligand; crystal structures of [WPt(μ-$CC_6H_3Me_2$-2,6)$(CO)_n(PEt_3)(\mu$-σ:η^5-$C_2B_9H_8Me_2)$](n= 2 or 3). *J. Chem. Soc., Dalton Trans.* **1989,** (2), 303-311 DOI: 10.1039/dt9890000303; (d) Lavallo, V.; Canac, Y.; DeHope, A.; Donnadieu, B.; Bertrand, G. A Rigid Cyclic (Alkyl)(amino)carbene Ligand Leads to Isolation of Low-Coordinate Transition-Metal Complexes. *Angew. Chem., Int. Ed. Engl.* **2005,** 44 (44), 7236-7239 DOI: 10.1002/anie.200502566.

8. Farrugia, L. J. WinGX and ORTEP for Windows: an update. *J. Appl. Crystallogr.* **2012,** 45, 849-854 DOI: 10.1107/S0021889812029111.

9. (a) Orpen, A. G. Indirect location of hydride ligands in metal cluster complexes. *J. Chem. Soc., Dalton Trans.* **1980,** (12), 2509-2516 DOI: 10.1039/dt9800002509; (b) Orpen, A. G.; Brammer, L.; Allen, F. H.; Kennard, O.; Watson, D. G.; Taylor, R. Supplement. Tables of bond lengths determined by X-ray and neutron diffraction. Part 2. Organometallic compounds and co-ordination complexes of the d- and f-block metals. *J. Chem. Soc., Dalton Trans.* **1989,** (12), S1-S83 DOI: 10.1039/dt98900000s1.

10. (a) Bould, J.; Harrington, R. W.; Clegg, W.; Kennedy, J. D. Nine-vertex metallaborane chemistry. Preparation and characterisation of 1,1,1-$(PMe_3)_2$-H-*isocloso*-IrB_8H_7-8-X , where X = H or Cl. *J. Organomet. Chem.* **2012,** 721, 155-163 DOI: 10.1016/j.jorganchem.2012.08.012; (b) Bould, J.; Clegg, W.; Kennedy, J. D. Polyhedral iridaborane chemistry: Elements of the 10-vertex *closo-isonido-isocloso* continuum molecular structures of $(PPh_3)_2HIrB_9H_9(PPh_3)$, $(PPh_3)(Ph_2PC_6H_4)IrB_9H_7(PPh_3)$, $(PPh_3)(Ph_2PC_6H_4)HIrB_9H_6Cl(PPh_3)$, $(PPh_3)(Ph_2PC_6H_4)HIrB_9H_6(PPh_3)_2$ and $(PPh_3)(Ph_2PC_6H_4)HIrB_9H_{12}$. *Inorg. Chim. Acta* **2006,** 359 (11), 3723-3735 DOI: 10.1016/j.ica.2006.01.038.

11. (a) Mantina, M.; Chamberlin, A. C.; Valero, R.; Cramer, C. J.; Truhlar, D. G. Consistent van der Waals Radii for the Whole Main Group. *J. Phys. Chem. A* **2009,** 113 (19), 5806-5812 DOI: 10.1021/jp8111556; (b) Alvarez, S. A cartography of the van der Waals territories. *Dalton Trans.* **2013,** 42 (24), 8617-8636 DOI: 10.1039/c3dt50599e; (c) We note that these M-μH-B type of interactions have often been described, by many authors, as 'agostic' (for example reference 14). However, the coiners of

the term object to this, saying, "this is an inappropriate use of the term agostic, which refers specifically to 3-center–2-electron interactions involving M–H–C groups, and does not refer to all 3-center–2-electron interactions." (Brookhart, M.; Green, M.L.H.; Parkin, G. *P Natl Acad Sci USA* **2007**, 104 (17), 6908–6914). We therefore avoid its use here. See Kennedy, J. D.; *J. Chem. Soc., Dalton Trans*. **1993**, (16), 2545-2546.

12. Yang, X.; Knobler, C. B.; Hawthorne, M. F. Macrocyclic Lewis acid host - halide ion guest species. Complexes of iodide ion. *J. Am. Chem. Soc.* **1992,** 114 (1), 380-382 DOI: 10.1021/ja00027a069.

13. Harwell, D. E.; McMillan, J.; Knobler, C. B.; Hawthorne, M. F. Structural Characterization of Representative d^7, d^8, and d^9 Transition Metal Complexes of Bis(o-carborane). *Inorg. Chem.* **1997,** 36 (25), 5951-5955 DOI: 10.1021/ic9706313.

14. Wang, Y.-P.; Zhang, L.; Lin, Y.-J.; Li, Z.-H.; Jin, G.-X. Selective B(4)−H Activation of an *o*-Carboranylthioamide Based on a Palladium Precursor. *Chem. Eur. J.* **2017,** 23 (8), 1814-1819 DOI: 10.1002/chem.201603851.

15. Bould, J.; Císařová, I.; Kennedy, J. D. Polyhedral Platinaborane Chemistry. Interaction of PMe_2Ph with $[(PMe_2Ph)_2PtB_{10}H_{12}]$. *Organometallics* **2012,** 31 (7), 2691-2696 DOI: 10.1021/om200940h.

16. Heintz, R. A.; Smith, J. A.; Szalay, P. S.; Weisgerber, A.; Dunbar, K. R. In *Inorg. Synth.*; Coucouvanis, D., Ed.; John Wiley & Sons, Inc.: 2002; Chapter 2, Vol. 33, pp 75-83.

17. Bould, J.; Clegg, W.; D. Kennedy, J.; J. Teat, S. Macropolyhedral boron-containing cluster chemistry. Mixed and multiple cluster fusion in platinaborane chemistry and the structure of $[(PMe_2Ph)_2PtB_{16}H_{17}PtB_{10}H_{11}(PMe_2Ph)]$ as determined by synchrotron X-ray diffraction analysis. *J. Chem. Soc., Dalton Trans.* **1998,** (17), 2777-2778.

18. Blandford, I.; Jeffery, J. C.; Jelliss, P. A.; Stone, F. G. A. Synthesis and Crystal Structure of the Novel Dianion $[Re(CO)_3(\eta^5\text{-}7\text{-}CB_{10}H_{11})]^{2-}$. Reactions with Platina- and Palladaphosphine Chlorides. *Organometallics* **1998,** 17 (7), 1402-1411 DOI: 10.1021/om9709143.

19. (a) Wade, K. In *Adv. Inorg. Chem. Radiochem.*; Emeléus, H. J., Sharpe, A. G., Ed.; Academic Press: 1976; Vol. 18, pp 1-66; (b) Wade, K. *J. Chem. Soc., Chem. Commun.* **1971**, 792.

20. Williams, R. E. Carboranes and boranes; polyhedra and polyhedral fragments. *Inorg. Chem.* **1971,** 10 (1), 210-214 DOI: 10.1021/ic50095a046.

21. Cordero, B.; Gómez, V.; Platero-Prats, A. E.; Revés, M.; Echeverría, J.; Cremades, E.; Barragán, F.; Alvarez, S. Covalent radii revisited. *Dalton Trans.* **2008,** (21), 2832-2838 DOI: 10.1039/b801115j.

22. Fletcher, D. A.; McMeeking, R. F.; Parkin, D. The United Kingdom Chemical Database Service. *J. Chem. Inform. Comput. Sci.* **1996,** 36 (4), 746-749 DOI: 10.1021/ci960015+.

23. (a) Ferguson, G.; Lough, A. J.; Faridoon; McGrath, M. N.; Spalding, T. R.; Kennedy, J. D.; Fontaine, X. L. R. Metallaheteroborane chemistry. Part 7. Synthesis, crystal structure, and

characterisation of two dinuclear rhodatelluraboranes, [{$(PPh_3)_2RhTeB_{10}H_{10}$}$_2$] and [$(PPh_3)(CO)Rh_2Te_2B_{20}H_{20}$]. *J. Chem. Soc., Dalton Trans.* **1990,** (6), 1831-1839 DOI: 10.1039/dt9900001831; (b) Jeffery, J. C.; Jelliss, P. A.; Lebedev, V. N.; Stone, F. G. A. Monocarbollide Complexes of Rhodium. *Organometallics* **1996,** 15 (22), 4737-4746 DOI: 10.1021/om9604435; (c) Wesemann, L.; Ramjoie, Y.; Ganter, B.; Wrackmeyer, B. The First Transition Metal Complex of a Silaborane. *Angew. Chem., Int. Edit. Engl.* **1997,** 36 (8), 888-890 DOI: 10.1002/anie.199708881; (d) Carr, N.; Mullica, D. F.; Sappenfield, E. L.; Stone, F. G. A. Carborane Complexes of Nickel and Platinum: Synthesis and Protonation Reactions of Anionic Allyl(carborane) Species. *Inorg. Chem.* **1994,** 33 (8), 1666-1673 DOI: 10.1021/ic00086a017; (e) Behnken, P. E.; Knobler, C. B.; Hawthorne, M. F. Synthesis and Structure Determination of $[(PEt_3)RhC_2B_9H_{10}]^{2-}$ A Binuclear Rhodacarborane Containing Four Bonds Betweeen Two Icosahedra. *Angew. Chem., Int. Edit. Engl.* **1983,** 22 (9), 722-723 DOI: 10.1002/anie.198307221; (f) Behnken, P. E.; Marder, T. B.; Baker, R. T.; Knobler, C. B.; Thompson, M. R.; Hawthorne, M. F. Synthesis, structural characterization, and stereospecificity in the formation of bimetallic rhodacarborane clusters containing rhodium-hydrogen-boron bridge interactions. *J. Am. Chem. Soc.* **1985,** 107 (4), 932-940 DOI: 10.1021/ja00290a031; (g) Hendershot, S. L.; Jeffery, J. C.; Jelliss, P. A.; Mullica, D. F.; Sappenfield, E. L.; Stone, F. G. A. Reaction of *nido*-7,8-$C_2B_9H_{13}$ with Dicobalt Octacarbonyl: Crystal Structures of the Complexes [$Co_2(CO)_2(\eta^5$-7,8-$C_2B_9H_{11})_2$], [$Co_2(CO)(PMe_2Ph)(\eta^5$-7,8-$C_2B_9H_{11})_2$], and [$CoCl(PMe_2Ph)_2(\eta^5$-7,8-$C_2B_9H_{11})$]. *Inorg. Chem.* **1996,** 35 (22), 6561-6570 DOI: 10.1021/ic960560s.

24. Bould, J.; Kennedy, J. D. Macropolyhedral boron-containing cluster chemistry. Novel intercluster linkages from the reaction of [Pt(cod)Cl_2] and [$PtMe_2(PMe_2Ph)_2$] with 6,6′-$(B_{10}H_{13})_2O$. *Chem. Commun.* **2007,** (47), 5084-5086 DOI: 10.1039/b712084b.

25. Nakashima, H.; Hasegawa, J.-Y.; Nakatsuji, H. On the reversible O_2 binding of the Fe–porphyrin complex. *J Comput Chem* **2006,** 27 (4), 426-433 DOI: 10.1002/jcc.20339.

26. Petříček, V.; Dušek, M.; Palatinus, L. Crystallographic Computing System JANA2006: General features. *Z. Anorg. Allg. Chem.* **2014,** 229 (5), 345 DOI: 10.1515/zkri-2014-1737.

TOC - Table of Contents

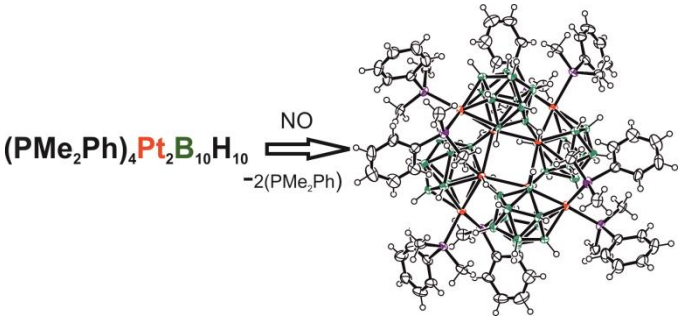

Synopsis

The propensity of the bimetalladocaborane cluster $(PMe_2Ph)_2Pt_2B_{10}H_{10}$ to reversibly sequester small molecules was tested with nitric oxide but, in the event, it unexpectedly afforded yields, by the simple loss of phosphine ligands, of cluster conglomerates in which a central core of up to 8 platinum atoms are held together by multicentre bonding. The molecule may be quantitatively disassembled by the addition of the isonitrile ligand EtNC.